

■ Supramolecular Optical Indicators

[2]Pseudorotaxane-Based Supramolecular Optical Indicator for the Visual Detection of Cellular Cyanide Excretion

Jiong Zhou,^[a] Guocan Yu,^{*[a]} Yang Li,^[b] Jie Shen,^[c] Mengbin Wang,^[a] Zhengtao Li,^[a] Peifa Wei,^[a] Jianbin Tang,^{*[d]} and Feihe Huang^{*[a]}

Abstract: Cyanide is extremely hazardous to living organisms and the environment. Owing to its wide range of applications and high toxicity, the development of functional materials for cyanide detection and sensing is highly desirable. Host–guest complexation between bis(*p*-phenylene)-34-crown-10 **H** and *N*-methylacridinium salt **G** remarkably decreases the detection limit for cyanide anions compared with that of the guest itself. The [2]pseudorotaxane selec-

tively recognizes the cyanide anion with high optical sensitivity as a result of the nucleophilic addition of the cyanide anion at the 9-position of **G**. The host–guest complexation is further incorporated into supramolecular materials for the visual detection of cyanide anions, especially the detection of cellular cyanide excretion with a detection limit of 0.6 μM. This supramolecular method provides an extremely distinct strategy for the visual detection of cyanide anions.

Introduction

Anion recognition is of particular interest, as it is involved in a wide range of chemical, biological, and environmental processes.^[1,2] The cyanide anion is extremely hazardous to living organisms and the environment.^[3,4] Owing to its wide range of applications and high toxicity, the development of functional materials for cyanide detection and sensing is highly desirable. Nucleophilic addition reactions of cyanide to acridine derivatives that possess suitable signaling properties have been used for the design of fluorescent chemosensors.^[5] However, owing to the π – π stacking of individual *N*-methylacridinium salts, the cyanide sensitivity is low. This is not good for cellular cyanide

detection, which is very important for instantaneous diagnosis and treatment of cyanide poisoning, and needs high sensitivity, as the cellular cyanide concentration is very low.^[4] Host–guest interactions play a significant role in the development of advanced supramolecular aggregates owing to their good selectivity and diverse responsiveness.^[6–13] Therefore, we anticipate that the utilization of host–guest interactions to inhibit intermolecular π – π stacking of *N*-methylacridinium salts will provide an excellent platform for the development of supramolecular materials for the visual detection of cyanide with high sensitivity.

As the star compounds in host–guest chemistry, the syntheses of crown ethers proclaimed the birth of supramolecular chemistry.^[14–22] Crown ether-based stimuli-responsive host–guest systems are very attractive and have been widely used in various areas.^[23–28] However, crown ether-based host–guest complexation for the visual detection of cyanide anions, especially the detection of cellular cyanide excretion, has not been reported yet. Herein, we develop a cyanide-responsive host–guest recognition motif between bis(*p*-phenylene)-34-crown-10 **H** and *N*-methylacridinium salt **G** (Figure 1). Interestingly, this host–guest complexation was responsive to cyanide anions. We demonstrated that the formation of the host–guest complex decreased the detection limit for CN[−] compared with that of the guest. Moreover, owing to its selectivity and sensitivity, the cyanide-responsive [2]pseudorotaxane is a perfect indicator that can be incorporated into functional supramolecular materials for the visual detection of cyanide anions, especially the detection of cellular cyanide excretion with a detection limit of 0.6 μM.

[a] Dr. J. Zhou, Dr. G. Yu, M. Wang, Dr. Z. Li, Dr. P. Wei, Prof. Dr. F. Huang
State Key Laboratory of Chemical Engineering
Center for Chemistry of High-Performance & Novel Materials
Department of Chemistry, Zhejiang University
Hangzhou 310027 (P. R. China)
E-mail: guocanyu@zju.edu.cn
fhuang@zju.edu.cn

[b] Y. Li
Department of Chemistry, Institute of Chemical Biology and
Pharmaceutical Chemistry, Zhejiang University
Hangzhou 310027 (P. R. China)

[c] J. Shen
School of Medicine, Zhejiang University City College
Hangzhou 310015 (P. R. China)

[d] Prof. Dr. J. Tang
Center for Bionanoengineering and Key Laboratory of
Biomass Chemical Engineering of Ministry of Education, College of
Chemical and Biological Engineering, Zhejiang University
Hangzhou 310027 (P. R. China)
E-mail: jianbin@zju.edu.cn

Supporting information and the ORCID identification number(s) for the author(s) of this article can be found under:
<https://doi.org/10.1002/chem.201903577>.

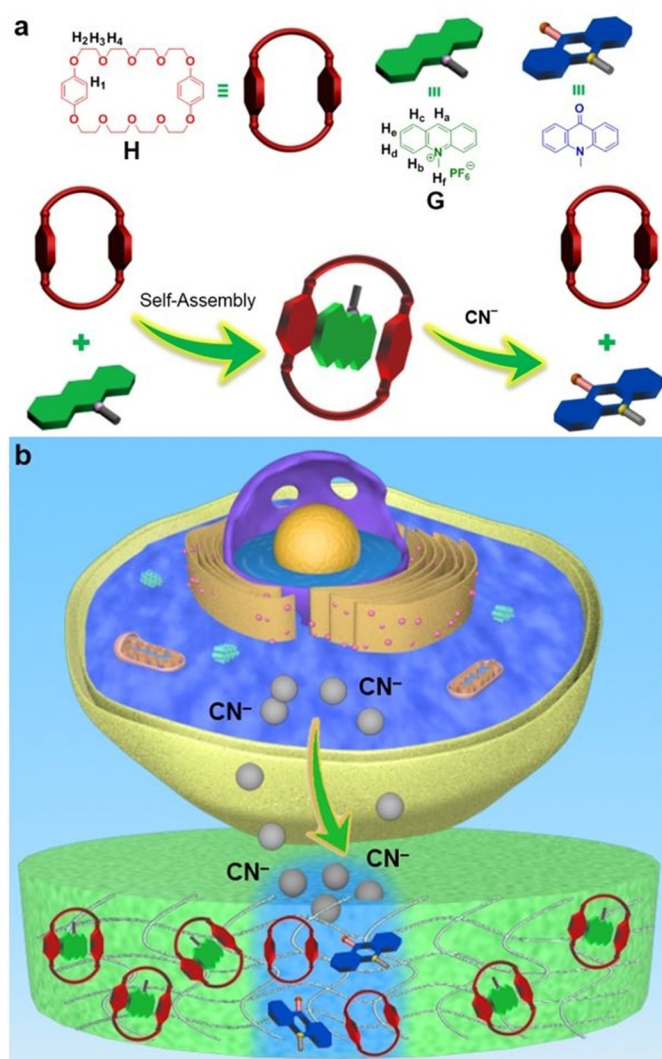


Figure 1. Schematic diagrams of the [2]pseudorotaxane serving as a cyanide-responsive supramolecular optical indicator platform. (a) Structures and cartoon representations of **H**, **G**, and cyanide-responsive [2]pseudorotaxane. (b) Cartoon representation of the visual detection of cyanide anion excreted from cells.

Results and Discussion

Host–guest interactions between **H** and **G**

The complexation between **H** and **G** was first investigated by ^1H NMR spectroscopy in acetone. The ^1H NMR spectrum (Figure 2b) of an equimolar solution of **H** and **G** in $[\text{D}_6]\text{acetone}$ displayed only one group of resonance peaks, indicating fast exchange complexation on the ^1H NMR timescale.^[22] In comparison with free **G**, the signals corresponding to protons H_a , H_b , and H_f of **G** exhibited upfield shifts ($\Delta\delta = -0.06$, -0.04 , -0.04 ppm for H_a , H_b , and H_f , respectively), providing convincing evidence for the interactions between **H** and **G**. In addition, protons on **H** also exhibited chemical shift changes (Figures 2b,d). The peak related to proton H_1 on the aromatic ring shifted upfield from 6.78 to 6.66 ppm owing to the interactions between **H** and **G**. To measure the binding affinity of the host–guest complexation, ^1H NMR titration experiments were con-

ducted at room temperature in $[\text{D}_6]\text{acetone}$. On the basis of the chemical shift changes of H_1 on **H** (Figure 3), the association constant (K_a) for $\text{H} \rightarrow \text{G}$ was calculated to be $(6.73 \pm 0.16) \times 10^2 \text{ m}^{-1}$ by employing a nonlinear curve-fitting method (Figure S4 in the Supporting Information). Furthermore, the complexation stoichiometry was determined to be 1:1 from the molar ratio plot (Figure S5 in the Supporting Information).

Additionally, the formation of the host–guest complex between **H** and **G** was validated by electrospray ionization mass spectroscopy (ESI-MS; Figure S7 in the Supporting Information). The ESI-MS spectrum of an equimolar mixture of **H** and **G** gave a mass fragment peak at $m/z = 730.2$, corresponding to $[\text{H} \rightarrow \text{G} \cdot \text{PF}_6]^{+}$, which further testified to the formation of the 1:1 complex of **H** with **G**, in agreement with the results obtained from ^1H NMR titrations.

Crystal structure

To precisely clarify how the host interacted with the guest, a single crystal of $\text{H} \rightarrow \text{G}$ suitable for X-ray analysis was obtained by slow diffusion of isopropyl ether into an equimolar acetone solution of **H** and **G** at room temperature. The crystal structure of $\text{H} \rightarrow \text{G}$ demonstrated that host **H** and guest **G** formed a [2]pseudorotaxane, driven by hydrogen bonding and face-to-face π -stacking interactions (Figure 4). Two hydrogen bonds (a, b) formed between two methyl hydrogen atoms of **G** and two ether oxygen atoms on **H**. Furthermore, a water molecule acted as a hydrogen bonding bridge between host **H** and guest **G**.

Detection of CN^- and reaction kinetics

Interestingly, the [2]pseudorotaxane exhibited cyanide responsiveness as a result of the nucleophilic addition of cyanide at the 9-position of **G**.^[5] The reaction of *N*-methylacridinium salt with cyanide anions produces *N*-methyl-9-cyanoacridan. In the presence of oxygen, *N*-methylacridone is subsequently yielded. This process induces a large decrease in fluorescence intensity and a marked color change. The cyanide-responsive property was confirmed by ^1H NMR spectroscopy (Figure 2c). Upon addition of CN^- (1.00 equiv) to a solution of $\text{H} \rightarrow \text{G}$, the ^1H NMR signal attributed to H_a of **G** disappeared, indicating that the nucleophilic addition of cyanide at the 9-position of **G** occurred. The peaks corresponding to protons on **H** returned to their original positions as free **H**. Meanwhile, when CN^- (1.00 equiv) was added into a solution of **G**, chemical shift changes related to the protons of **G** behaved the same as the solution of $\text{H} \rightarrow \text{G}$ in which CN^- (1.00 equiv) was added, demonstrating that there was no complexation between **H** and the nucleophilic addition reaction product (Figures S37 and S38 in the Supporting Information). Furthermore, photographs of the solution of the inclusion complex between **H** and **G** before and after adding CN^- verify its cyanide-responsiveness (Figure S39 in the Supporting Information). When an equimolar acetone solution of **H** was mixed with **G**, a brick-red color appeared immediately owing to the host–guest interactions between **H** and **G**. However, the color of the mixture changed to

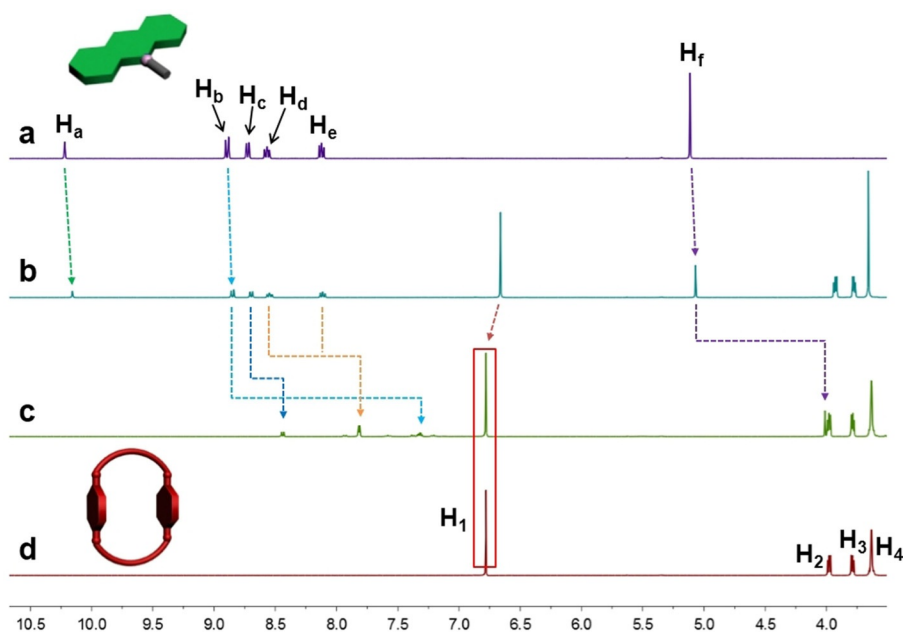


Figure 2. Partial ^1H NMR spectra (400 MHz, $[\text{D}_6]$ acetone, 293 K): (a) 5.00 mM **G**; (b) 5.00 mM **H** and 5.00 mM **G**; (c) after addition of tetrabutylammonium cyanide (CN^-) (1.00 equiv) to b; (d) 5.00 mM **H**.

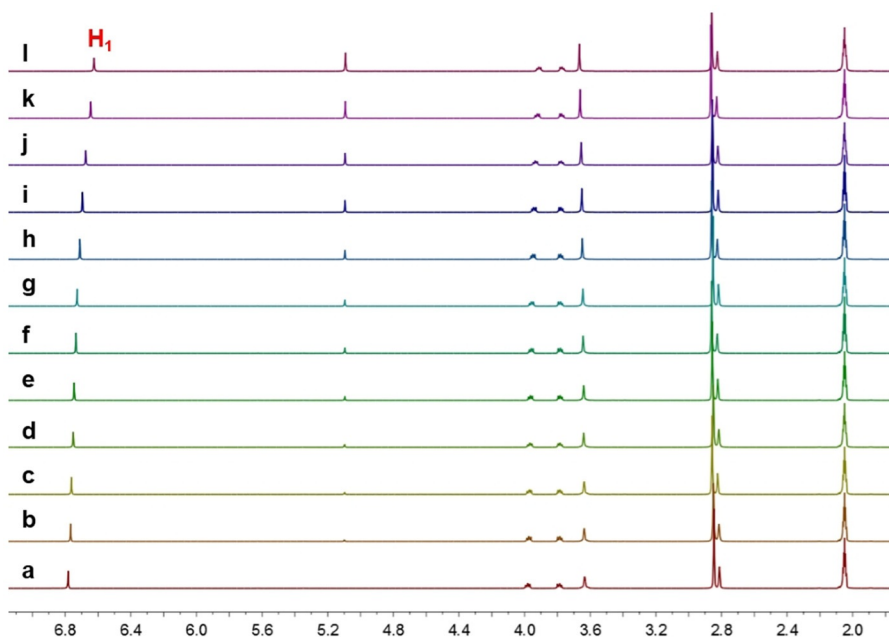


Figure 3. Partial ^1H NMR spectra (400 MHz, $[\text{D}_6]$ acetone, 293 K) of **H** at a concentration of 2.00 mM upon addition of **G**: (a) 0.00 mM; (b) 0.840 mM; (c) 1.07 mM; (d) 1.64 mM; (e) 1.73 mM; (f) 2.27 mM; (g) 2.70 mM; (h) 3.50 mM; (i) 4.40 mM; (j) 5.63 mM; (k) 7.16 mM; (l) 8.43 mM.

olive by the addition of cyanide anion. Undoubtedly, this supramolecular system can be used in the construction of cyanide-responsive chemosensors.

The solubility of individual *N*-methylacridinium salts in aqueous solution is extremely poor, arising from the π - π stacking, significantly lowering its sensitivity.^[3] This limitation could be solved by fully taking advantage of supramolecular chemistry. The K_a value for **H** \supset **G** was calculated to be $(1.44 \pm 0.51) \times$

10^5 M^{-1} in water from isothermal titration calorimetry (ITC; Figure S6 in the Supporting Information), which was much higher than the corresponding K_a value in acetone owing to hydrophobic interactions.^[6] Meanwhile, the formation of the host-guest complex between **H** and **G** in water was validated by ESI-MS (Figure S8 in the Supporting Information). To further investigate the interaction between [2]pseudorotaxane **H** \supset **G** and CN^- , fluorescence spectral variations of **H** \supset **G** and **G** were

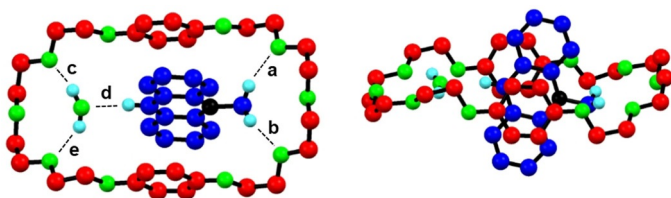


Figure 4. Two views of the X-ray crystal structure of $\text{H}\supset\text{G}$. Host H is red, guest G is blue, hydrogen atoms are sky blue, oxygen atoms are green, and nitrogen atoms are black. The PF_6^- counterion, solvent molecules, and hydrogens except the ones on G and a water molecule involved in hydrogen bonding are omitted for clarity. Parameters related to non-covalent interactions between H and G are shown in Tables S1 and S2 (in the Supporting Information).

monitored during titration with CN^- (Figure 5 and Figures S9–S28 in the Supporting Information). Addition of CN^- resulted in a drastic decrease in the peak at 491 nm, and the appear-

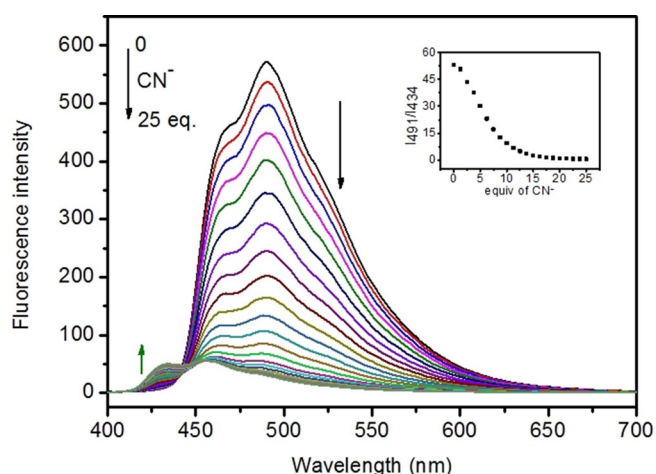


Figure 5. Fluorescence spectra of $\text{H}\supset\text{G}$ ($10.0\ \mu\text{M}$) upon addition of TBACN in water ($\lambda_{\text{ex}} = 358\ \text{nm}$). Inset: plot of the fluorescent intensity ratio change at 491 nm and 434 nm (I_{491}/I_{434}) of $\text{H}\supset\text{G}$ as a function of CN^- concentration.

ance of a new peak at 434 nm, accompanied by a fluorescent color change from cyan to blue (Figure 6a). The new peak considerably increased with the gradual addition of CN^- , and a well-defined isoemissive point appeared at 445 nm. The cyanide anion detection limit was determined to be $19.0\ \text{nm}$ with a linear ratio response (I_{491}/I_{434}) of the fluorescence intensity to cyanide concentration (Figures S21 and S22 in the Supporting Information). It should be pointed out that the detection limit of $\text{H}\supset\text{G}$ was much lower than that of the free guest (Figures S13 and S14 in the Supporting Information), emphasizing the role that the host–guest complexation played in improving the sensitivity. The detection limit was not influenced by changing the solution pH (Figures S13–S28 in the Supporting Information). The low detection limit suggests [2]pseudorotaxane $\text{H}\supset\text{G}$ can be used to detect whether the level of CN^- in drinking water exceeds $1.9\ \mu\text{M}$ (the World Health Organization standard).^[29] Furthermore, the time-dependent changes in the absorption spectra and the emission spectra of $\text{H}\supset\text{G}$ and G upon the addition of cyanide were almost complete within 15 min (Figures S29–S36 in the Supporting Information).

To investigate the CN^- selectivity of $\text{H}\supset\text{G}$, we carried out a series of ion recognition experiments. The recognition profiles of $\text{H}\supset\text{G}$ toward various ions, including CN^- , F^- , Cl^- , Br^- , I^- , NO_3^- , SCN^- , AcO^- , ClO_4^- , HSO_4^- , H_2PO_4^- , and SO_4^{2-} ions (tetrabutylammonium salts), were investigated by exciting the corresponding solutions at 358 nm and measuring the emission in water (Figure 6a). When 50 equivalents of CN^- were added to an aqueous solution of $\text{H}\supset\text{G}$, the fluorescence emission intensity at 491 nm rapidly decreased to a fundamentally minimum constant value. The apparent fluorescence emission changed from cyan to blue as distinguished by the naked eye. To validate the selectivity of $\text{H}\supset\text{G}$, competitive tests were also conducted by using F^- , Cl^- , Br^- , I^- , NO_3^- , SCN^- , AcO^- , ClO_4^- , HSO_4^- , H_2PO_4^- , and SO_4^{2-} ions, and none of these ions induced a significant fluorescence change in the emission peak at 491 nm (Figure 6a). The fluorescence data revealed that $\text{H}\supset\text{G}$ was highly selective toward CN^- over the other common

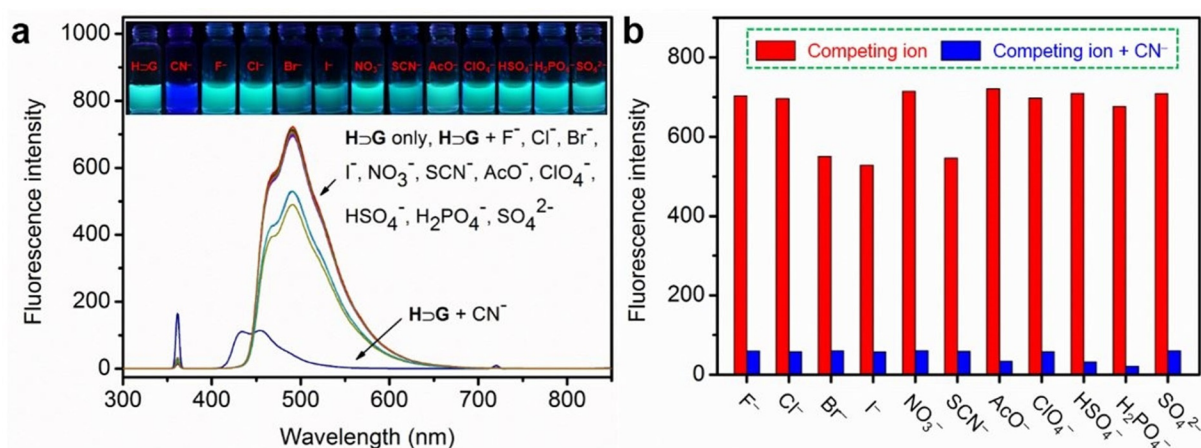


Figure 6. (a) Fluorescence spectral responses of $\text{H}\supset\text{G}$ ($10.0\ \mu\text{M}$) in water upon addition of 50 equivalents of CN^- , F^- , Cl^- , Br^- , I^- , NO_3^- , SCN^- , AcO^- , ClO_4^- , HSO_4^- , H_2PO_4^- , and SO_4^{2-} ions (tetrabutylammonium salts) ($\lambda_{\text{ex}} = 358\ \text{nm}$). Inset: photograph of $\text{H}\supset\text{G}$ ($10.0\ \mu\text{M}$) under a UV lamp (365 nm) upon adding 50 equivalents of various ions. (b) Fluorescence intensity changes of $\text{H}\supset\text{G}$ ($10.0\ \mu\text{M}$) in the presence of 50 equivalents of various ions after addition of 50 equivalents of CN^- in water ($\lambda = 491\ \text{nm}$).

anions, owing to the fact that cyanide is more nucleophilic than the other anions. These results indicated that **H**⊃**G** may have application in the detection of cyanide anions in the presence of other anions. To explore the utility of **H**⊃**G** as an ion-selective chemosensor for CN^- , competitive experiments were carried out in the presence of 50 equivalents of CN^- and 50 equivalents of various other ions (F^- , Cl^- , Br^- , I^- , NO_3^- , SCN^- , AcO^- , ClO_4^- , HSO_4^- , H_2PO_4^- , and SO_4^{2-}) in water (Figure 6b). The results of these studies revealed that these competing ions exerted no or little influence on the fluorescence emission spectra of **H**⊃**G** with CN^- , which further indicated that **H**⊃**G** has specific selectivity for CN^- .

Sensing properties of **H**⊃**G** in industrial and biological applications

In gold and silver mining, cyanide is used to recover the precious metals through a leaching process.^[30] Typically, dilute solutions of sodium cyanide, normally in the range of 0.2–1 mM% cyanide, are used in tank leaching and heap leaching processes. In the majority of these cases, cyanide from processing operations enters the environment either by leakage through tears and/or punctures in the protective heap leach liners, or by spillage from overflowing solution ponds or tailings storage areas. To explore the industrial application of the cyanide-responsive [2]pseudorotaxane, a model was prepared by cutting agarose gels doped with a solution of **H**⊃**G** (1.00×10^{-5} M). Upon the addition of CN^- (1.00×10^{-4} M) to the gel of **H**⊃**G**, the fluorescent color changed from cyan to blue under 365 nm UV light (Figure S40 in the Supporting Information). Similarly, a test strip or a thin film was prepared to sense CN^- , and the fluorescent color change was also visualized (Figure S41 in the Supporting Information). When CN^- was added onto these solid supported materials, nucleophilic addition of cyanide at the 9-position of **G** occurred and the host–guest complexation between **H** and **G** was disrupted, accompanied by changes in fluorescent color. Therefore, the easy-to-make device could be a convenient test kit for detecting CN^- in the industrial field.

The excellent selectivity of **H**⊃**G** for CN^- over other anions in aqueous media indicates its utility for biological applications. Cyanide can bind heme cofactors to inhibit the terminal respiratory chain enzyme cytochrome C oxidase.^[4] The development of a real-time detection method for cellular cyanide excretion is thus of great importance. The cytotoxicities of **H**, **G**, and **H**⊃**G** against HEK293 cells were evaluated by a 3-(4',5'-dimethylthiazol-2'-yl)-2,5-diphenyltetrazolium bromide (MTT) assay (Figure S43 in the Supporting Information). Negligible changes in relative cell viability were observed for the cells cultured with **H**⊃**G** even at a high concentration, indicating the biocompatibility of this supramolecular system, enabling **H**⊃**G** to serve as a potential probe for fluorescence sensing of intracellular CN^- .

Time-dependent fluorescence color changes of a supramolecular hydrogel containing **H**⊃**G** were recorded, triggered by various concentrations of CN^- (Figure S42 in the Supporting Information). Prior to the cyanide addition, **H**⊃**G** exhibited a cyan color. When CN^- was added, a clear color change from

cyan to blue was observed. More excitingly, this supramolecular material was utilized to visually detect the cyanide anion excreted from the cells (Figure 7). After culturing the cells in a medium containing different concentrations of CN^- for 24 h, the cells were harvested and further cultured on the surface of a supramolecular hydrogel containing 2% **H**⊃**G** to visualize the excretion of CN^- . The excreted CN^- permeated the supramolecular gels and reacted with the indicator. As a consequence, the fluorescent color of the supramolecular gel changed from cyan to blue. As shown in Figure 7, the detection limit of this supramolecular system was as low as 0.6 μM .

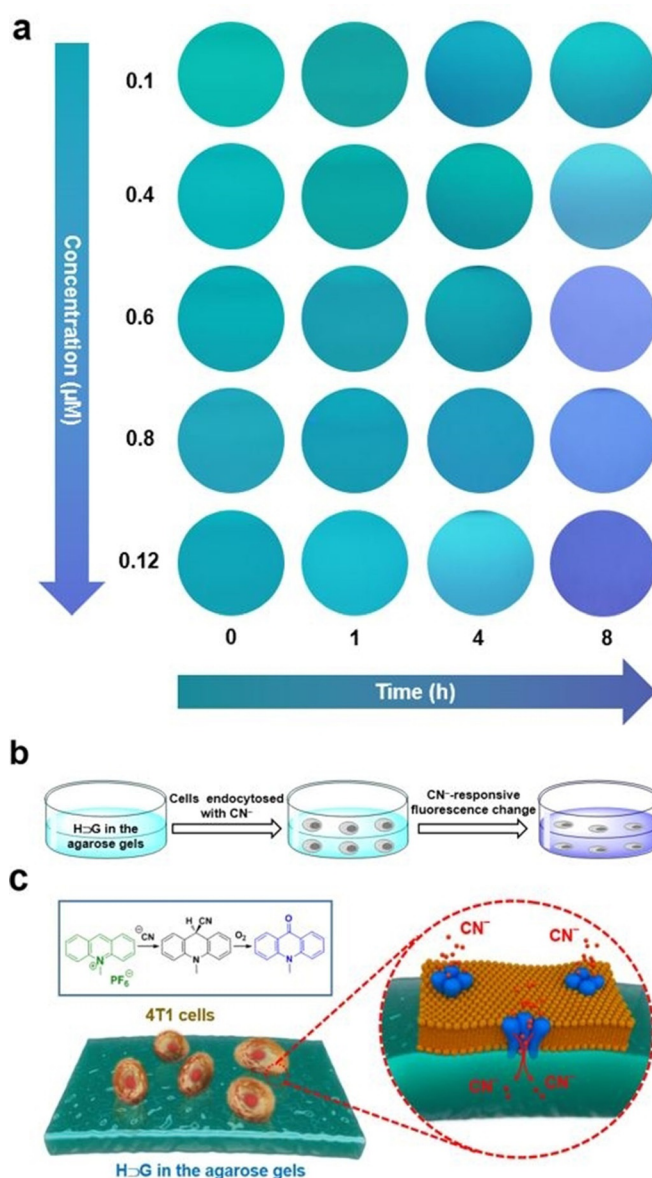


Figure 7. (a) CN^- -responsive fluorescence color change of **H**⊃**G** in the agarose gels incubated with 4T1 cells for varying times. (b, c) Schematic illustration of the CN^- -responsive behavior.

Conclusion

We demonstrated that the host–guest complexation between **H** and **G** remarkably decreased the detection limit for CN^- compared with that of the guest alone. From **H** and **G**, a [2]pseudorotaxane formed driven by hydrogen bonding and face-to-face π -stacking interactions. Interestingly, this host–guest complexation was responsive to CN^- . Moreover, the cyanide-responsive [2]pseudorotaxane was developed into supramolecular materials for the visual detection of cyanide anions, especially the detection of cellular cyanide excretion with a detection limit of 0.6 μM . This cyanide-responsive binding property is a novel feature of the host–guest properties of bis(*p*-phenylene)-34-crown-10. More importantly, this cyanide-responsive host–guest complex holds promising potential in biomedical applications such as disease-specific biomarker detection and early-stage precise diagnosis.

Experimental Section

Procedures for anion sensing

Stock solutions of CN^- , F^- , Cl^- , Br^- , I^- , NO_3^- , SCN^- , AcO^- , ClO_4^- , HSO_4^- , H_2PO_4^- , and SO_4^{2-} (5.00 mM) were prepared from their tetrabutylammonium (TBA) salts. Solutions of **G** (10.0 μM) and **H**⊃**G** (10.0 μM) were prepared in water. The sensing of CN^- by **G** and **H**⊃**G** were performed by adding the TBACN stock solution by means of a micro-pipette to 2.00 mL of a solution of **G** or **H**⊃**G**. Test samples for selectivity experiments were prepared by adding appropriate amounts of stock solutions of anions (tetrabutylammonium salts) with a similar procedure. In competition experiments, TBACN was added to solutions containing **G** and **H**⊃**G** and the other anions of interest. All test solutions were stirred for 20 min at room temperature. For all fluorescence experiments, excitation was fixed at 358 nm, and fluorescence emission was collected from 300 to 850 nm.

Cell culture

A549, HEK293, and 4T1 cells were cultured in Dulbecco's modified Eagle's medium (DMEM) containing 10% fetal bovine serum (FBS) and 1% penicillin/streptomycin. Cells grew as a monolayer and were detached upon confluence by using trypsin (0.5% w/v in PBS). The cells were harvested from cell culture medium by incubating in a trypsin solution for 5 min. The cells were centrifuged, and the supernatant was discarded. A 3 mL portion of serum-supplemented DMEM was added to neutralize any residual trypsin. The cells were resuspended in serum-supplemented DMEM at a concentration of 1×10^4 cells mL^{-1} . Cells were cultured at 37 °C and 5% CO_2 .

Cytotoxicity evaluation

The cytotoxicities of **H**, **G**, **H**⊃**G**, and CN^- against A549, HEK293, and 4T1 cells were determined by 3-(4',5'-dimethylthiazol-2'-yl)-2,5-diphenyltetrazolium bromide (MTT) assays in a 96-well cell culture plate. All solutions were sterilized by filtration through a 0.22 μm filter before tests. A549, HEK293, and 4T1 cells were seeded at a density of 1×10^4 cells/well in a 96-well plate, and incubated for 18 h for attachment. Cells were then incubated with **H**, **G**, **H**⊃**G**, and TBACN at various concentrations for 24 h. After washing the cells with PBS buffer, 100 μL of a MTT solution (0.5 mg mL^{-1}) was

added to each well. After 4 h of incubation at 37 °C, the MTT solution was removed, and the insoluble formazan crystals that formed were dissolved in dimethylsulfoxide (DMSO, 100 μL). The absorbance of the formazan product was measured at 570 nm by using a spectrophotometer (Bio-Rad Model 680). Untreated cells in the medium were used as a control. All experiments were carried out with five replicates.

The 4T1 cells were seeded at a density of 16×10^4 cells/well in a 6-well plate, and incubated for 18 h for attachment. Cells were then incubated with TBACN at various concentrations for 24 h. After incubation, the cells were washed with PBS, trypsinized, re-suspended in sterile water (2 mL). Then, the cells were repeatedly frozen, sonicated, and broken. The concentration of CN^- in the cells was measured by using a CN^- detection kit (HKM, China) in accordance with the manufacturer's protocol. This concentration was calculated according to the color chart; the total number of cells was 3 million and the volume was 10 mL in the whole system. The CN^- detection experiments were done under physiological conditions.

CCDC 1510444 contains the supplementary crystallographic data for this paper. These data are provided free of charge by The Cambridge Crystallographic Data Centre.

Acknowledgments

This work was supported by the National Natural Science Foundation of China (21434005, 91527301).

Conflict of interest

The authors declare no conflict of interest.

Keywords: cellular cyanide excretion • crown compounds • pseudorotaxane • supramolecular optical indicators • visual detection

- [1] a) P. D. Beer, P. A. Gale, *Angew. Chem. Int. Ed.* **2001**, *40*, 486; *Angew. Chem. Int. Ed.* **2001**, *113*, 502; b) N. H. Evans, P. D. Beer, *Angew. Chem. Int. Ed.* **2014**, *53*, 11716; *Angew. Chem.* **2014**, *126*, 11908; c) N. Busschaert, C. Caltagirone, W. V. Rossom, P. A. Gale, *Chem. Rev.* **2015**, *115*, 8038.
- [2] Z. Zhang, D. S. Kim, C.-Y. Lin, H. Zhang, A. D. Lammer, V. M. Lynch, I. Popov, O. Š. Miljanić, E. V. Anslyn, J. L. Sessler, *J. Am. Chem. Soc.* **2015**, *137*, 7769.
- [3] a) Z. Xu, X. Chen, H. N. Kim, J. Yoon, *Chem. Soc. Rev.* **2010**, *39*, 127; b) Z. Guo, S. Park, J. Yoon, I. Shin, *Chem. Soc. Rev.* **2014**, *43*, 16; c) M. H. Lee, J. S. Kim, J. L. Sessler, *Chem. Soc. Rev.* **2015**, *44*, 4185; d) P. A. Gale, C. Caltagirone, *Chem. Soc. Rev.* **2015**, *44*, 4212; e) L. You, D. Zha, E. V. Anslyn, *Chem. Rev.* **2015**, *115*, 7840; f) Q. He, G. I. Vargas-Zúñiga, S. H. Kim, S. K. Kim, J. L. Sessler, *Chem. Rev.* **2019**, *119*, 9753.
- [4] F. Wang, L. Wang, X. Chen, J. Yoon, *Chem. Soc. Rev.* **2014**, *43*, 4312.
- [5] Y.-K. Yang, J. Tae, *Org. Lett.* **2006**, *8*, 5721.
- [6] N. L. Strutt, R. S. Forgan, J. M. Spruell, Y. Y. Botros, J. F. Stoddart, *J. Am. Chem. Soc.* **2011**, *133*, 5668.
- [7] X.-D. Xu, X. Li, H. Chen, Q. Qu, L. Zhao, H. Ågren, Y. Zhao, *Small* **2015**, *11*, 5901.
- [8] a) C. Talotta, C. Gaeta, Z. Qi, C. A. Schalley, P. Neri, *Angew. Chem. Int. Ed.* **2013**, *52*, 7437; *Angew. Chem.* **2013**, *125*, 7585; b) W. Wang, L.-J. Chen, X.-Q. Wang, B. Sun, X. Li, Y. Zhang, J. Shi, Y. Yu, L. Zhang, M. Liu, H.-B. Yang, *Proc. Natl. Acad. Sci. USA* **2015**, *112*, 5597; c) A. J. McConnell, C. S. Wood, P. P. Neelakandan, J. R. Nitschke, *Chem. Rev.* **2015**, *115*, 7729.
- [9] Z. He, W. Jiang, C. A. Schalley, *Chem. Soc. Rev.* **2015**, *44*, 779.
- [10] a) Y. Sun, J. Ma, F. Zhang, F. Zhu, Y. Mei, L. Liu, D. Tian, H. Li, *Nat. Commun.* **2017**, *8*, 260; b) M.-X. Wu, J. Gao, F. Wang, J. Yang, N. Song, X. Jin, P. Mi, J. Tian, J. Luo, F. Liang, Y.-W. Yang, *Small* **2018**, *14*, 1704440;

- c) B. Li, B. Wang, X. Huang, L. Dai, L. Cui, J. Li, X. Jia, C. Li, *Angew. Chem. Int. Ed.* **2019**, *58*, 3885; *Angew. Chem.* **2019**, *131*, 3925.
- [11] a) G. Yu, X. Zhao, J. Zhou, Z. Mao, X. Huang, Z. Wang, B. Hua, Y. Liu, F. Zhang, Z. He, O. Jacobson, C. Gao, W. Wang, C. Yu, X. Zhu, F. Huang, X. Chen, *J. Am. Chem. Soc.* **2018**, *140*, 8005; b) X. Li, Z. Li, Y.-W. Yang, *Adv. Mater.* **2018**, *30*, 1800177; c) J. Zhou, Y. Zhang, G. Yu, M. R. Crawley, C. R. P. Fulong, A. E. Friedman, S. Sengupta, J. Sun, Q. Li, F. Huang, T. R. Cook, *J. Am. Chem. Soc.* **2018**, *140*, 7730.
- [12] M. Zuo, W. Qian, Z. Xu, W. Shao, X.-Y. Hu, D. Zhang, J. Jiang, X. Sun, L. Wang, *Small* **2018**, *14*, 1801942.
- [13] X.-Q. Wang, W. Wang, W.-J. Li, L.-J. Chen, R. Yao, G.-Q. Yin, Y.-X. Wang, Y. Zhang, J. Huang, H. Tan, Y. Yu, X. Li, L. Xu, H.-B. Yang, *Nat. Commun.* **2018**, *9*, 3190.
- [14] a) C. O. Dietrich-Buchecker, J.-P. Sauvage, *Chem. Rev.* **1987**, *87*, 795; b) D. B. Amabilino, J. F. Stoddart, *Chem. Rev.* **1995**, *95*, 2725; c) K. Kinbara, T. Aida, *Chem. Rev.* **2005**, *105*, 1377.
- [15] a) W. R. Browne, B. L. Feringa, *Nat. Nanotechnol.* **2006**, *1*, 25; b) Z. Niu, H. W. Gibson, *Chem. Rev.* **2009**, *109*, 6024; c) K. Zhu, V. N. Vukotic, S. J. Loeb, *Angew. Chem. Int. Ed.* **2012**, *51*, 2168; *Angew. Chem.* **2012**, *124*, 2210.
- [16] a) Y. Han, Z. Meng, Y.-X. Ma, C.-F. Chen, *Acc. Chem. Res.* **2014**, *47*, 2026; b) T. L. Price, Jr., H. W. Gibson, *J. Am. Chem. Soc.* **2018**, *140*, 4455.
- [17] a) S. Erbas-Cakmak, D. A. Leigh, C. T. McTernan, A. L. Nussbaumer, *Chem. Rev.* **2015**, *115*, 10081; b) J. Zhou, G. Yu, F. Huang, *Chem. Soc. Rev.* **2017**, *46*, 7021.
- [18] K. Zhu, C. A. O'Keefe, V. N. Vukotic, R. W. Schurko, S. J. Loeb, *Nat. Chem.* **2015**, *7*, 514.
- [19] S.-L. Li, T. Xiao, C. Lin, L. Wang, *Chem. Soc. Rev.* **2012**, *41*, 5950.
- [20] D.-H. Qu, Q.-C. Wang, Q.-W. Zhang, X. Ma, H. Tian, *Chem. Rev.* **2015**, *115*, 7543.
- [21] X. Ma, Y. Zhao, *Chem. Rev.* **2015**, *115*, 7794.
- [22] H. R. Wessels, C. Slebodnick, H. W. Gibson, *J. Am. Chem. Soc.* **2018**, *140*, 7358.
- [23] J. Li, D. Yim, W.-D. Jang, J. Yoon, *Chem. Soc. Rev.* **2017**, *46*, 2437.
- [24] a) L. Chen, Y.-K. Tian, Y. Ding, Y.-J. Tian, F. Wang, *Macromolecules* **2012**, *45*, 8412; b) S. Li, J. Huang, T. R. Cook, J. B. Pollock, H. Kim, K.-W. Chi, P. J. Stang, *J. Am. Chem. Soc.* **2013**, *135*, 2084; c) J.-F. Xu, Y.-Z. Chen, D. Wu, L.-Z. Wu, C.-H. Tung, Q.-Z. Yang, *Angew. Chem. Int. Ed.* **2013**, *52*, 9738; *Angew. Chem.* **2013**, *125*, 9920; d) X.-Y. Hu, T. Xiao, C. Lin, F. Huang, L. Wang, *Acc. Chem. Res.* **2014**, *47*, 2041; e) L. Yang, X. Tan, Z. Wang, X. Zhang, *Chem. Rev.* **2015**, *115*, 7196.
- [25] a) L. Isaacs, *Acc. Chem. Res.* **2014**, *47*, 2052; b) M. Xue, Y. Yang, X. Chi, X. Yan, F. Huang, *Chem. Rev.* **2015**, *115*, 7398.
- [26] F. Würthner, C. R. Saha-Möller, B. Fimmel, S. Ogi, P. Leowanawat, D. Schmidt, *Chem. Rev.* **2016**, *116*, 962.
- [27] D. B. Amabilino, D. K. Smith, J. W. Steed, *Chem. Soc. Rev.* **2017**, *46*, 2404.
- [28] a) Y. Zhou, H.-Y. Zhang, Z.-Y. Zhang, Y. Liu, *J. Am. Chem. Soc.* **2017**, *139*, 7168; b) L. K. S. von Krbek, D. A. Roberts, B. S. Pilgrim, C. A. Schalley, J. R. Nitschke, *Angew. Chem. Int. Ed.* **2018**, *57*, 14121; *Angew. Chem.* **2018**, *130*, 14317.
- [29] D. Shan, C. Mousty, S. Cosnier, *Anal. Chem.* **2004**, *76*, 178.
- [30] G. Hilson, A. J. Monhemius, *J. Cleaner Prod.* **2006**, *14*, 1158.

Manuscript received: August 5, 2019

Accepted manuscript online: September 8, 2019

Version of record online: October 16, 2019